Journal of Materials and Environmental Science
ISSN : 2028-2508
CODEN : JMESCN

J. Mater. Environ. Sci., 2026, Volume 17, Issue 4, Page 590-605

http://www.jmaterenvironsci.com

Preparation and Study of the Physical and Mechanical Properties of Ceramic Membranes from Syrian Fly Ash (Class C) for Drinking Water Treatment

Abdulrazzaq Hammal[1]*, Mohamad Saleh Faleh[2]

[1] *Department of Basic Science (Chemistry), Faculty of Electrical Engineering, University of Aleppo, Aleppo, Syria*
[2] *Department of Basic Science (Physics), Faculty of Electrical Engineering, University of Aleppo, Aleppo, Syria*

Corresponding author: ab.hammal@alepuniv.edu.sy

Received 15 Feb 2026,
Revised 07 Apr 2026,
Accepted 08 Apr 2026

Keywords
- ✓ *Fly ash,*
- ✓ *Ceramic membranes,*
- ✓ *Physical properties,*
- ✓ *Boric acid,*
- ✓ *Water treatment,*
- ✓ *Microfiltration.*

Citation: *Hammal A. and Faleh M.S. (2026), Preparation and Study of the Physical and Mechanical Properties of Ceramic Membranes from Syrian Fly Ash (Class C) for Drinking Water Treatment, J. Mater. Environ. Sci., 17(4), pp. 590-605.*

Abstract: Low-cost ceramic membranes were prepared from Syrian fly ash (Class C) using boric acid (0-7.5%) as a binder. The raw material was characterized by XRF and XRD, confirming its classification as Class C (ASTM C618) with 16.80% CaO and 62.10% (SiO_2+Al_2O_3+Fe_2O_3). Major crystalline phases identified were quartz and calcite, along with an amorphous glassy phase. Membranes were fabricated by uniaxial pressing (600 kg/cm²) and sintered at 900°C. The addition of boric acid up to 5% significantly improved the properties: apparent porosity decreased from 38.75% to 26.80%, bulk density increased from 1.58 to 2.08 g/cm³, Vickers hardness increased from 2280 to 3670 MPa, and compressive strength increased from 15.8 to 31.4 MPa. Permeability decreased from 0.045 to 0.009 Darcy. The 7.5% addition caused partial melting, establishing 5% as the optimal ratio. The B5 membrane showed high efficiency in drinking water treatment, reducing turbidity from 12.80 to 2.50 NTU (80.5% removal), suspended solids from 25 to 3 mg/L (88%), COD from 32 to 3 mg/L (90.6%), and BOD_5 from 19 to 2 mg/L (89.5%), meeting Syrian drinking water standards. The membranes showed no significant TDS reduction due to their microfiltration nature. These results demonstrate that Syrian fly ash is a promising low-cost material for producing effective ceramic membranes, achieving dual objectives of industrial waste recycling and high-value product development.

1. Introduction

Water is an indispensable vital resource for life, and securing it in sufficient quantities and to appropriate quality is one of the most prominent global challenges facing humanity in the twenty-first century. This goal is directly linked to achieving the United Nations Sustainable Development Goals (Obaideen *et al.,* 2022). Rapid industrialization and population growth have generated huge quantities of wastewater and industrial effluents laden with various and dangerous pollutants, posing a serious threat to aquatic ecosystems and public health worldwide (Sawunyama *et al.,* 2024; Jones *et al.,* 2022). Reports indicate that more than 50-80% of wastewater is discharged into the environment without adequate treatment, necessitating the development of effective, robust, and low-cost treatment technologies (Jones *et al.,* 2022; Friesen *et al.,* 2023).

Membrane filtration technology has emerged as one of the most effective methods in water treatment due to its high separation efficiency, small footprint, and ability to produce high-quality water (Dong

et al., 2022). Ceramic membranes, in particular, have clear advantages compared to their polymeric counterparts, including superior chemical and thermal stability, high mechanical strength, long operational life, and excellent resistance to harsh operating conditions, making them suitable for treating challenging water types (Samadi *et al.,* 2022; Asif & Zhang, 2021). However, the widespread application of these membranes on an industrial scale is often hindered by the high cost of traditional raw materials (such as alumina, zirconia, or titania), which range between 500-1000 USD per square meter, in addition to energy-intensive manufacturing processes requiring high sintering temperatures up to 1300-1700°C (Asif & Zhang, 2021; Sawunyama *et al.,* 2024b). This situation has stimulated researchers to explore low-cost and environmentally friendly alternatives, such as natural minerals and industrial wastes rich in silicon and aluminum oxides, for manufacturing these membranes (Abdullayev *et al.,* 2019; Goswami *et al.,* 2022).

Coal fly ash is one of the most important promising industrial wastes. It is a by-product of pulverized coal combustion in thermal power plants and is produced in huge quantities estimated at hundreds of millions of tons annually worldwide (Hossain & Roy, 2020; Gollakota *et al.,* 2019). Fly ash consists mainly of silicon oxide (SiO_2), aluminum oxide (Al_2O_3), iron oxide (Fe_2O_3), and calcium oxide (CaO). It is characterized by fine spherical granular shape and amorphous structure that gives it pozzolanic activity (Wang *et al.,* 2021; Jin *et al.,* 2020). The disposal of this waste poses a significant environmental burden due to its content of toxic heavy elements that may leach into soil and groundwater and pollute the air, making its recycling a primary goal for sustainable development and the circular economy (Mushtaq *et al.,* 2019; Labidi *et al.,* 2023).

According to the American Standard Specification ASTM C618, fly ash is classified into Class F and Class C. Class **C** fly ash is characterized by a high percentage of calcium oxide (CaO) (more than 10%), which gives it pozzolanic and self-cementing properties. The presence of free lime allows it to react directly with water to form calcium silicate hydrates (CSH), which may contribute to the bonding process between particles and lower the sintering temperature required for membrane preparation (ASTM C618-19; Adewuyi, 2021). Studies have shown that using fly ash in the preparation of ceramic membranes can significantly reduce production costs to as low as 17-250 USD per square meter, compared to traditional commercial membranes (Sawunyama *et al.,* 2024; Singh & Bulasara, 2015).

Previous studies have demonstrated the possibility of using various local materials to prepare effective ceramic membranes for water treatment. In the field of pharmaceutical wastewater treatment, geopolymer membranes were prepared from Syrian clay reinforced with industrial wastes (refractory bricks, ceramics, and glass). These membranes showed high efficiency in removing organic load, with COD removal reaching 95.74% and bacterial pollutant removal reaching 99.5% (Hammal, 2025). Ceramic membranes were also successfully prepared from raw Syrian zeolite impregnated with silver nanoparticles and proved effective in treating well water by reducing chemical index values (COD by 96.9%, BOD by 95.45%) and almost completely eliminating bacterial pollutants (Hammal, 2023). These results indicate the great potential of local Syrian raw materials and wastes in this field.

The properties and performance of ceramic membranes prepared from fly ash are affected by several factors including sintering temperature, proportion of binders and fluxing agents, type and quantity of pore-forming materials, and particle size of the raw material (Liang *et al.,* 2021; Huang *et al.,* 2023). Studies have shown that adding materials such as boric acid (H_3BO_3) can act as a binder and fluxing agent, as it melts at a relatively low temperature (about 170°C) to form a liquid glassy phase that spreads between particles, increases interparticle bonding, and improves mechanical properties.

However, excessive addition leads to partial melting and deformation of the sample (Agarwal *et al.,* 2020; Suresh *et al.,* 2016).

Although there are numerous global studies on the use of fly ash in the preparation of ceramic membranes (Sawunyama *et al.,* 2024a; Samadi *et al.,* 2022; Goswami *et al.,* 2022), they have mainly focused on the use of traditional binders such as sodium silicate (Cui et al., 2023), polyvinyl alcohol (Das & Kayal, 2023; Fu *et al.,* 2022; Jiang *et al.,* 2018), carboxymethyl cellulose (Liang *et al.,* 2021; Huang *et al.,* 2022), and corn starch (Liang *et al.,* 2021; Huang *et al.,* 2022). In contrast, none of the previous studies—to the best of available information—have addressed the use of boric acid (H_3BO_3) as a binder and fluxing agent in the preparation of ceramic membranes from fly ash, especially Class C. The use of boric acid in the few studies has been limited to its role as a dispersant to improve mixture homogeneity rather than a primary binder (Singh & Bulasara, 2015; Agarwal *et al.,* 2020). The scientific literature also lacks studies on the potential use of Syrian fly ash (from Banias Refinery) in this field, creating a clear knowledge gap that this research seeks to fill.

The importance of this research stems from being the first of its kind to study the effect of adding boric acid in different proportions (0%, 2.5%, 5%, 7.5%) on the physical and mechanical properties of ceramic membranes prepared from fly ash, while determining the optimal ratio that achieves the best balance between suitable porosity for filtration and adequate mechanical strength. In addition, the research contributes to recycling Syrian fly ash (an industrial waste that accumulates in large quantities) and converting it into a high-value-added material (ceramic membranes) for drinking water treatment, achieving the dual goals of protecting the environment from pollution and providing low-cost local solutions to water pollution problems.

2. Methodology

2.1 Characterization of Fly Ash

Samples of fly ash used in this study were collected from the electrostatic precipitators of the Banias Refinery (Tartous Governorate, Syria). This ash represents industrial waste resulting from the combustion of sub-bituminous coal in power generation units. The samples were initially dried in an air oven (Memmert UN55, Germany) at 105 ± 5°C for 24 hours to remove surface and free moisture, then sieved using a standard sieve with a 200 µm opening (Retsch AS 200, Germany) to obtain a fine and homogeneous powder, and stored in airtight polyethylene containers until use.

Chemical analysis of fly ash was performed using an X-ray fluorescence spectrometer (XRF, model: PANalytical Axios, Netherlands). To prepare the sample for analysis, 10 g of dried fly ash was mixed with 3 g of boric acid (H_3BO_3, purity ≥ 99.5%, Merck, Germany) as a binder. The mixture was placed in an aluminum mold and pressed using a hydraulic press (Specac, UK) with a force of 150 kN to obtain a compressed disc with a diameter of 30 mm and a thickness of 5 mm. The disc was then transferred to the analysis chamber, and the device was operated at 50 kV voltage and 50 mA current. The percentages of oxides were estimated using the qualitative analysis software attached to the device, based on the standard calibration method.

The results—presented in **Table 1**—show that the sample contains a high percentage of calcium oxide (CaO) at 16.80%, and the total of acidic oxides (SiO_2 + Al_2O_3 + Fe_2O_3) is 62.10%, which is less than 70%, confirming that this ash is classified as Class C according to the American Standard Specification ASTM C618. This class is characterized by having pozzolanic and self-cementing properties due to its high calcium content, which may contribute to lowering the sintering temperature during the preparation of ceramic membranes.

Table 1. Chemical composition of the studied fly ash by XRF technique

Component	Percentage (%)
SiO_2	42.30
Al_2O_3	14.80
Fe_2O_3	5.00
CaO	16.80
MgO	4.50
SO_3	2.10
K_2O	0.90
Na_2O	0.60
Loss on Ignition (L.O.I)	2.80
Total	99.80

Phase analysis of fly ash was performed using an X-ray diffraction device (XRD, model: PANalytical X'Pert Pro, Netherlands) to identify the main crystalline phases. The fine powder was placed in a glass sample holder and smoothed well to obtain a flat surface, then inserted into the analysis chamber. The device was operated at 40 kV voltage and 30 mA current, using CuKα radiation (wavelength 1.5406 Å) with a nickel filter. Diffraction patterns were recorded in the 2θ angular range between 5° and 70° with a step size of 0.02°. Crystalline phases were identified by comparing the resulting diffraction peaks with reference database cards (ICDD) using HighScore Plus software.

The results showed a mixture of crystalline phases, most notably quartz (SiO_2) and calcite ($CaCO_3$), in addition to possible secondary phases such as hematite (Fe_2O_3) and mullite ($3Al_2O_3 \cdot 2SiO_2$), with an amorphous glassy phase represented by a broad hump in the angular range of 20-35°.

2.2 Preparation of Inorganic Membranes from Fly Ash

2.2.1 Preparation of Mixtures and Mixing

Four mixtures of fly ash with different weight percentages of boric acid (H_3BO_3, purity ≥ 99.5%, Merck, Germany) were prepared as follows:

i. **B0:** Reference sample: 50 g fly ash + 0 g boric acid (0% ratio)
ii. **B2.5:** 48.75 g fly ash + 1.25 g boric acid (2.5% ratio)
iii. **B5:** 47.5 g fly ash + 2.5 g boric acid (5% ratio)
iv. **B7.5:** 46.25 g fly ash + 3.75 g boric acid (7.5% ratio)

Materials were weighed using a sensitive electronic analytical balance (Sartorius CPA224S, Germany, reading accuracy ± 0.1 mg). Each mixture was dry-mixed in a porcelain ball mill (Retsch PM 400, Germany) equipped with a porcelain grinding jar and grinding balls of the same material with different diameters (10, 20, 30 mm). Dry mixing was carried out for 15 minutes at a rotation speed of 250 rpm to ensure complete homogeneity of the powders. After dry mixing, 5 mL of distilled water (local product, laboratory distillation unit, Faculty of Science, University of Aleppo) was added gradually with continued manual mixing to obtain a homogeneous and moldable paste.

2.2.2 Pressing and Shaping

The wet mixture was placed in a cylindrical stainless steel mold (locally designed and manufactured) with an internal diameter of 50 mm and distributed evenly throughout the mold. The mixture was then pressed using a manual uniaxial hydraulic press (Specac, UK) under a force of 600 kg/cm² (equivalent to 58.8 MPa) for a full two minutes to ensure cohesion of the green samples. After pressing, the samples were carefully removed as circular discs with a diameter of 50 mm and a thickness of 2.5 ± 0.2 mm.

The shaped samples were left to air-dry for 24 hours on clean shelves, then dried in an air drying oven (Memmert UN55, Germany) at 60°C for an additional 24 hours. The purpose of this stage was to gradually and slowly remove excess water to avoid cracks or warping in the samples before heat treatment.

2.2.3 Heat Treatment (Sintering)

The dried samples were placed in a high-temperature electric heat treatment furnace (Carbolite CWF 1300, UK), equipped with a programmable digital PID controller of the Eurotherm type. A controlled multi-stage thermal program was applied to the samples, designed based on the expected thermal characteristics of Class C fly ash (high calcium content and low L.O.I) and to ensure the removal of residual carbon and optimal sintering. The program included the following stages:

- **Initial heating and final drying stage:** From room temperature to 110°C at a slow heating rate of 2°C/min, with temperature held at 110°C for 60 minutes to expel any remaining moisture.
- **Carbon burning stage:** From 110°C to 600°C at a heating rate of 3°C/min, with a hold at 600°C for 120 minutes to ensure combustion of any remaining organic carbon (L.O.I is relatively low but present).
- **Boric acid melting stage:** From 600°C to 800°C at a heating rate of 3°C/min, with a hold for 30 minutes to ensure melting of boric acid and its distribution between particles.
- **Final sintering stage:** From 800°C to **900°C** at a heating rate of 5°C/min, with a hold at 900°C for 180 minutes. The maximum temperature was chosen as 900°C instead of 950°C or 1000°C due to the high percentage of calcium oxide (CaO), which acts as a flux and may cause early melting or deformations at higher temperatures.
- **Cooling stage:** Heating was stopped and the samples were left to cool gradually inside the furnace until reaching room temperature, to avoid thermal shock.

2.3 Characterization of Prepared Membranes

The physical and mechanical specifications of the membranes after sintering were determined using the following standard methods:

2.3.1 Apparent Porosity and Water Absorption Rate

This test was performed according to the standard method ASTM C373. The samples were dried in a drying oven (Memmert UN55) at 105°C until constant weight, and the dry weight (D) was recorded using an analytical balance (Sartorius). The samples were then immersed in distilled water and boiled for two hours, then left to cool and become saturated with water. After saturation, the saturated weight (W) was determined after gently wiping the surface, and the suspended weight (S) was determined by suspending the sample in water. Apparent porosity (P) and water absorption rate (A) were calculated from the following equations:

$$\mathbf{P\ (\%) = [(W - D) / (W - S)] \times 100}$$

$$\mathbf{A\ (\%) = [(W - D) / D] \times 100}$$

2.3.2 Bulk Density and Apparent Specific Gravity

Bulk density (B) and apparent specific gravity (T) were calculated from the following equations using the previous measurements:

$$\mathbf{B\ (g/cm^3) = D / (W - S)}$$

$$\mathbf{T = D / (D - S)}$$

2.3.3 Vickers Hardness

The hardness of the prepared membranes was measured using a Vickers hardness tester (Innovatest Nexus 4304, Netherlands). The device was equipped with a diamond pyramid with four faces at an angle of 136°. A load of 0.5 kgf (4.9 N) was applied to the polished surface of the sample for 15 seconds. The average length of the impression diagonals (D) was measured using the attached magnifying lens. The Vickers hardness value (HV) was calculated from the equation:

$$\mathbf{HV = 1.8544 \times P / D^2}$$

Where P is the applied load (kgf), and D is the average length of the impression diagonals (mm). Values were converted to MPa by multiplying the result by 9.807. Five readings were taken at different points on each sample, and the arithmetic mean was taken.

2.3.4 Compressive Strength

The compressive strength of the disc membranes was determined using a compressive strength testing machine (MATEST E161, Italy) equipped with a load cell with a capacity of 100 kN. The sample was placed between the device jaws, and an axial compressive force was applied at a constant loading speed of 0.5 mm/min until complete sample failure. The failure load (F) was recorded in Newtons, and the compressive strength (σ) was calculated in MPa from the equation:

$$\mathbf{\sigma\ (MPa) = F / A}$$

Where F is the failure load (N), and A is the cross-sectional area of the sample (m^2) (disc area = π × (radius)^2). The test was performed on three samples of each type, and the average was taken.

2.3.5 Permeability

The water permeability of the membranes was estimated using Darcy's Law. The membrane was fixed in a locally manufactured filtration cell, and distilled water was passed through the membrane under constant pressure (0.5 bar). The volumetric flow rate (Q) of water was measured in (m^3/s). Permeability (k) was calculated from the equation:

$$\mathbf{k = (Q \times \mu \times \Delta L) / (A \times \Delta P)}$$

Where:

- **k:** Permeability (Darcy, where 1 Darcy = 9.87×10^{-13} m^2)
- **μ:** Water viscosity (Pa·s, taken as 1×10^{-3} at 20°C)
- **ΔL:** Membrane thickness (m)
- **A:** Effective membrane surface area (m^2)
- **ΔP:** Pressure difference across the membrane (Pa)

2.4 Evaluation of Membrane Performance in Water Treatment

Raw water samples were collected from a water well located on the University of Aleppo campus (Faculty of Science) using clean 5 L polyethylene containers. The samples were preserved in a cooler (4°C) during transport and until analysis, and storage time did not exceed 48 hours.

The filtration process was carried out by fixing each membrane individually in the filtration cell and passing 1 L of raw water sample through the membrane under constant pressure (0.5 bar). The filtrate was collected, and the following indices were measured before and after filtration, with three measurements taken for each sample and the average value recorded:

Turbidity: Measured using a turbidity meter (HACH 2100P, USA) according to the nephelometric method (USEPA Method 180.1). The device was calibrated weekly using standard solutions (StabCal®).

True Color: Evaluated using a colorimeter (HACH DR/890, USA) at a wavelength of 420 nm, after removing turbidity by centrifugation. Results were expressed in Pt-Co units.

Suspended Solids (SS): Estimated using the same device (HACH DR/890) at a wavelength of 610 nm.

Chemical Oxygen Demand (COD): Determined by the digestion method. 2 mL of sample was added to an ampoule containing digestion solution (potassium dichromate), then placed in a COD reactor (HACH DRB 200, USA) at 150°C for two hours. After cooling, the sample was measured at a wavelength of 420 nm using a colorimeter (DR/890).

Biochemical Oxygen Demand (BOD_5): Measured using the OxiTop® system (WTW OxiTop® Control 6, Germany). The sample (432 mL) was placed in 500 mL amber bottles, and nitrification inhibitor ($C_4H_8N_2S$), nutrient buffer, and bacterial seed (Polyseed) were added. Pressure measuring heads were attached to the bottles and incubated in a special incubator (WTW TS 606) at 20 ± 1°C in the dark for 5 days. Readings were recorded directly in mg/L.

Total Dissolved Solids (TDS): Estimated indirectly by measuring electrical conductivity using a conductivity meter (JENWAY 470, UK). TDS value was calculated from the relationship: TDS (mg/L) = EC (µS/cm) × 0.65 (at 20°C).

3. Results and Discussion

3.1 Characterization of Fly Ash

3.1.1 Chemical Composition

The results of the chemical analysis of the studied fly ash, shown in **Table 1**, indicate that it contains silicon dioxide (SiO_2) at 42.30%, aluminum oxide (Al_2O_3) at 14.80%, and iron oxide (Fe_2O_3) at 5.00%, with the total of these three oxides being approximately 62.10%. The results also show that the sample contains a high percentage of calcium oxide (CaO) reaching 16.80%, in addition to other oxides in lower percentages such as magnesium oxide (MgO) at 4.50%, sulfur trioxide (SO_3) at 2.10%, and sodium and potassium oxides at 0.60% and 0.90%, respectively. The loss on ignition (L.O.I) was 2.80%, and the total sum was 99.80%.

These percentages indicate that the studied sample belongs to Class C according to the American Standard Specification ASTM C618, which stipulates that fly ash of this class should have a total acidic oxides ($SiO_2 + Al_2O_3 + Fe_2O_3$) between 50% and 70%, and the percentage of calcium oxide (CaO) should exceed 10%. This type of ash is characterized by pozzolanic and self-cementing properties due to its high calcium content, allowing it to react directly with water to form calcium silicate hydrates (CSH) and calcium aluminate hydrates (CAH). This property is expected to play an important role in the sintering process during membrane preparation, as it may help lower the required sintering temperature and increase interparticle bonding.

The presence of iron oxide (Fe_2O_3) at 5.00% is also noted, which can act as a flux and participate in forming low-melting glassy phases. The loss on ignition (L.O.I) of 2.80% indicates the presence of a small amount of unburned carbon or organic matter, an acceptable percentage that requires consideration during the design of the thermal program to ensure its removal before the completion of the sintering process.

3.1.2 Phase Composition

Figure 1 shows the X-ray diffraction (XRD) pattern of the studied fly ash in the 2θ angular range from 5° to 50°. The pattern shows characteristic diffraction peaks reflecting the main crystalline phases in the sample, along with a broad hump indicating an amorphous glassy phase. Crystalline phases were identified by comparing peak positions and diffraction angles with reference database cards (ICDD), results showed the presence of the following phases (**Table 2**):

Quartz (SiO_2)

Quartz appears as the main and most prominent crystalline phase in the sample through a highly distinct diffraction peak at an angle of **2θ ≈ 26.6°**, in addition to secondary peaks at angles **20.8°** and **50.1°**. The main quartz peak has the highest intensity in the pattern, indicating the abundance of this phase in the sample. Quartz is characterized by its high thermal stability and chemical resistance and contributes to forming the structural framework of fly ash and the membranes prepared from it.

Calcite ($CaCO_3$)

Calcite appears clearly through a medium-intensity diffraction peak at an angle of **2θ ≈ 29.5°**, which is the second most prominent peak in the pattern. The presence of calcite indicates that part of the calcium oxide in the ash is combined with carbon dioxide in the form of calcium carbonate. The presence of calcite is important for the following reasons:

At high temperatures (during the sintering process), calcite thermally decomposes to give calcium oxide (CaO) and carbon dioxide gas (CO_2), according to the equation: $\mathbf{CaCO_3 \rightarrow CaO + CO_2\uparrow}$

The release of CO_2 gas during sintering may contribute to the formation of additional porosity in the membrane structure. Calcium oxide resulting from decomposition can contribute to the self-cementing properties of the ash and react with silica and alumina to form bonding phases.

Other Possible Phases

In addition to the two main peaks of quartz and calcite, some small, low-intensity peaks appear in various angular ranges, most notably:

Low-intensity peaks at angles **33.1°** and **35.6°** that may belong to the **hematite** phase (Fe_2O_3), which is consistent with the presence of iron oxide in the chemical analysis (5.00%).

Faint peaks at angles **16.4°** and **40.8°** that may belong to the **mullite** phase ($3Al_2O_3 \cdot 2SiO_2$), which is less pronounced than in Class F ash due to the relatively lower alumina content.

Glassy Phase (Amorphous)

A broad hump (halo) is clearly observed at the base of the peaks within the 2θ angular range between **20° and 35°**, indicating the presence of an amorphous glassy phase in significant proportion in the sample. This glassy phase is primarily responsible for the pozzolanic activity of fly ash, as it reacts with calcium ions (resulting from calcite decomposition or originally present) in the aqueous medium to form additional binding materials. The presence of the glassy phase enhances the sinterability of the ash and the formation of coherent membranes at suitable temperatures.

Table 2. Main crystalline phases identified in the XRD pattern of fly ash

Crystalline Phase	Chemical Formula	2θ (°)	Peak Intensity
Quartz	SiO_2	20.8, 26.6, 50.1	Very high
Calcite	$CaCO_3$	29.5	Medium
Hematite*	Fe_2O_3	33.1, 35.6	Low
Mullite*	$3Al_2O_3 \cdot 2SiO_2$	16.4, 40.8	Low (faint)

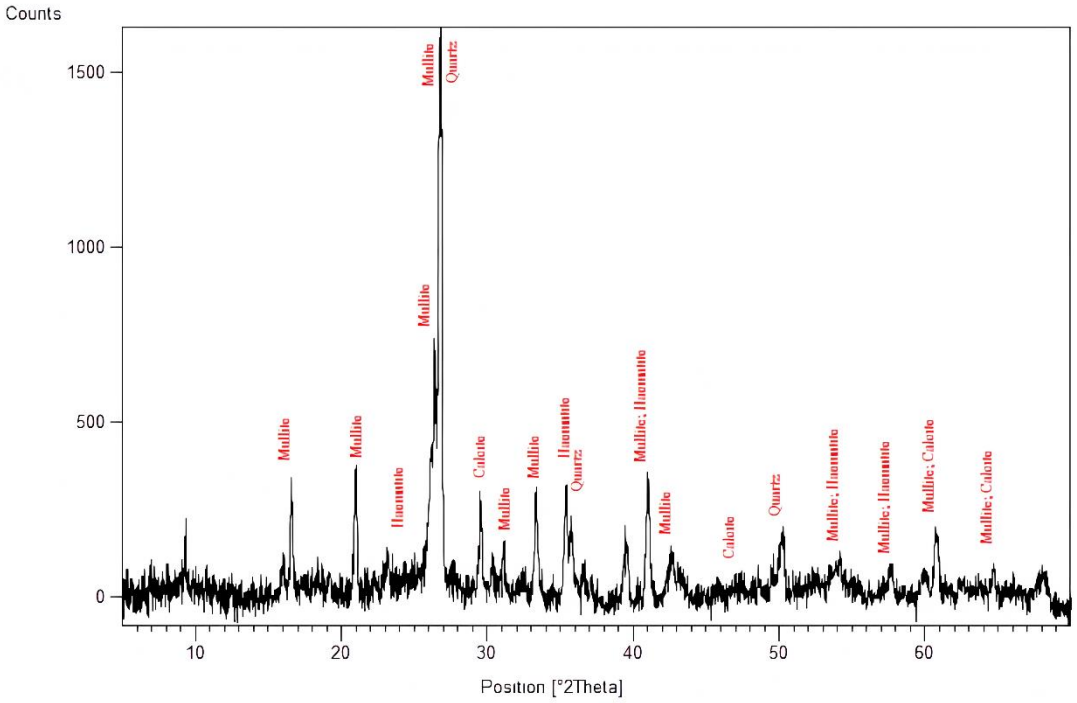

a

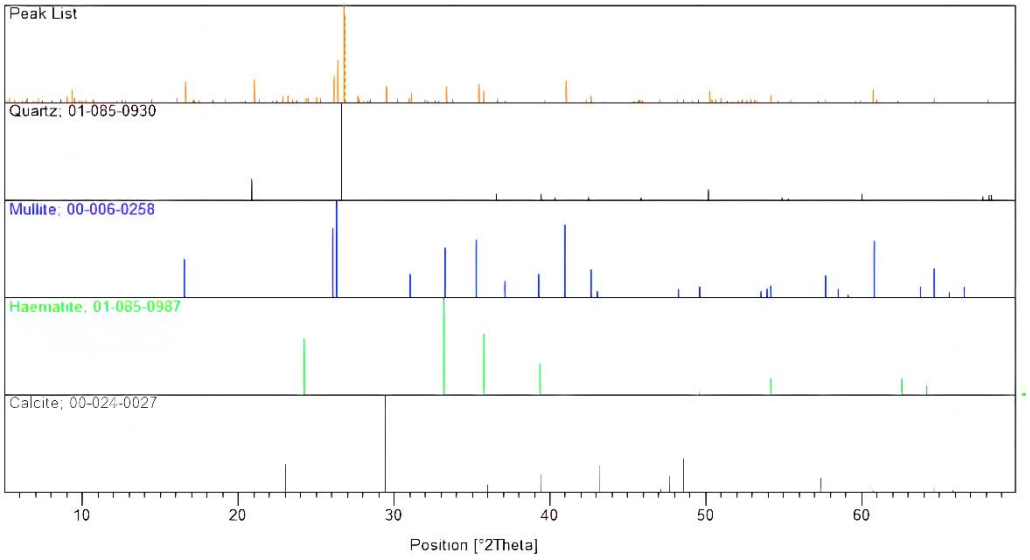

b

Figure 1. X-ray diffraction analysis of Syrian fly ash: (a) Full XRD pattern of the studied fly ash, (b) Reference ICDD patterns for the identified crystalline phases

These results indicate that the studied fly ash consists of a mixture of crystalline phases (most importantly quartz and calcite) alongside an amorphous glassy phase in significant proportion. This phase composition reflects the thermal conditions the coal was subjected to during combustion and directly affects the sample behavior during heat treatment. The presence of calcite in particular is an important indicator for anticipating the release of CO_2 gas during sintering, which may contribute to the formation of additional porosity in the prepared membranes, while quartz and the glassy phase contribute to enhancing mechanical properties and sinterability

3.2 Characterization of Membranes Prepared from Fly Ash

3.2.1 Physical Properties

Table 3 shows the main physical properties of the membranes prepared from fly ash with different proportions of boric acid after heat treatment at 900°C. The results clearly show the effect of boric acid on all the properties studied.

Table 3. Physical properties of membranes prepared from fly ash

Property	B0 (0% H_3BO_3)	B2.5 (2.5% H_3BO_3)	B5 (5% H_3BO_3)	B7.5 (7.5% H_3BO_3)
Apparent porosity (%)	38.75	32.45	26.80	Sample excluded*
Water absorption (%)	21.35	17.20	12.65	Sample excluded*
Bulk density (g/cm³)	1.58	1.82	2.08	Sample excluded*
Apparent specific gravity	1.95	2.32	2.65	Sample excluded*

**Sample B7.5 was excluded due to partial melting and clear deformation of the disc shape as a result of the increase in the fluxing agent.*

From the **Table 3**, we observe that apparent porosity decreases significantly with increasing boric acid proportion from 0% to 5%, decreasing from 38.75% to 26.80%, a reduction of about 31%. Conversely, bulk density increases from 1.58 g/cm³ to 2.08 g/cm³, and apparent specific gravity increases from 1.95 to 2.65. This behavior is due to the role of boric acid as a fluxing agent, as it melts at a relatively low temperature (about 170°C) to form a liquid glassy phase that spreads between fly ash particles. This glassy phase performs several functions:

First, it coats the ash particles and increases the contact area between them. Second, it spreads into the interparticle voids, reducing pore volume. Third, it lowers the sintering temperature required for neck formation between particles and increases the rate of atomic diffusion. As a result, particles bond more strongly, interparticle distances (pores) decrease, leading to increased density and decreased porosity and water absorption. For the B7.5 sample, partial melting and deformation of the disc shape were observed after heat treatment, leading to its exclusion from subsequent studies. This is because increasing the boric acid proportion beyond 5% led to the formation of a very large quantity of liquid glassy phase at 900°C, causing the sample to lose its geometric shape and collapse its porous structure. This indicates that the optimal proportion of boric acid is 5% by weight, where the best balance between mechanical cohesion and maintaining a suitable porous structure is achieved.

3.2.2 Mechanical Properties

Table 4 shows the mechanical properties of the prepared membranes, namely Vickers hardness and compressive strength. The results show a significant improvement in mechanical properties as the boric acid proportion increases. Vickers hardness increased from 2280 MPa for the B0 sample to 3670 MPa for the B5 sample, a 61 % increase. Similarly, compressive strength increased from 15.8 MPa to 31.4 MPa, an increase of about 99% (approximately double the value).

Table 4. Mechanical properties of membranes prepared from fly ash

Membrane	Vickers Hardness (MPa)	Compressive Strength (MPa)
B0	2280	15.8
B2.5	2980	22.5
B5	3670	31.4

This improvement reinforces the previous interpretation regarding the role of boric acid in enhancing sintering and increasing interparticle bonding. With increased sintering, the bonding strength between particles increases, and defects and voids, which constitute weak points in the structure, decrease, thereby improving the sample's resistance to mechanical forces (compression and hardness). Additionally, the glassy phase formed from boric acid has high hardness, thereby increasing the membrane's overall hardness. It is worth noting that the achieved compressive strength (31.4 MPa for the B5 sample) is acceptable for filtration membrane applications and is consistent with similar values in previous studies on ceramic membranes prepared from low-cost materials (Samadi *et al.,* 2022; Goswami *et al.,* 2022).

3.2.3 Permeability

Table 5 shows the permeability values of the prepared membranes measured in Darcy units. Permeability decreases significantly with increasing boric acid proportion, from 0.045 Darcy for the B0 sample to 0.009 Darcy for the B5 sample, a reduction of up to 80%. This decrease is a direct result of the decrease in apparent porosity as previously demonstrated. As porosity decreases, the pore channels become fewer and smaller, increasing resistance to water flow through the membrane. This behavior is expected and is consistent with Darcy's law, which relates permeability to the porosity of the porous medium and pore geometry. There is an inverse relationship between permeability and both porosity and compressive strength, as increasing mechanical cohesion (by increasing sintering) leads to reduced voids and consequently reduced permeability. This represents a well-known trade-off in filtration membranes, where a balance must be achieved between adequate mechanical strength and appropriate permeability for the required application.

Table 5. Permeability of membranes prepared from fly ash

Membrane	Permeability (Darcy)
B0	0.045
B2.5	0.021
B5	0.009

3.3 Effectiveness of Prepared Membranes in Drinking Water Treatment

The effectiveness of the prepared membranes (B0, B2.5, B5) was tested in treating raw water samples collected from a well at the University of Aleppo (Faculty of Science). **Table 6** shows the water specifications before and after the filtration process, compared with the Syrian standard specification (45/2007) for drinking water. The results show a clear effectiveness of the prepared membranes in improving water specifications, especially in removing turbidity, suspended solids, and organic pollutants. The results can be discussed as follows:

Turbidity and Suspended Solids

The membranes significantly reduced turbidity, decreasing from 12.80 NTU before treatment to 2.50 NTU after filtration with the B5 membrane, which is below the permissible limit in the Syrian standard (5 NTU). The turbidity removal rate for the B5 membrane reached approximately 80.5%. Similarly, suspended solids decreased from 25 mg/L to 3 mg/L, a removal rate of 88%. This high efficiency is attributed to the physical retention mechanism (mechanical filtration) by which the membranes operate, where the pore diameter of the membrane (related to total porosity) is smaller than the diameter of particles causing turbidity and suspended solids, leading to their retention on the membrane surface or

within its porous structure. We note that the removal efficiency increases with increasing boric acid proportion (B5 > B2.5 > B0), which corresponds to a decrease in porosity and an increase in compactness of the membrane's internal structure, as shown in **Table 3**.

Table 6. Water specifications before and after filtration with prepared membranes

Parameter	Unit	Syrian Standard	Before Treatment	B0	B2.5	B5
Turbidity	NTU	≤ 5	12.80	6.20	4.10	2.50
Suspended Solids (SS)	mg/L	≤ 10	25	12	6	3
Color	Pt-Co	≤ 15	12	9	6	4
COD	mg/L	≤ 3	32	14	6	3
BOD_5	mg/L	≤ 2	19	8	3	2
TDS	mg/L	≤ 1200	940	945	942	947

Color

The color value decreased from 12 Pt-Co before treatment to 4 Pt-Co after filtration with the B5 membrane, which is lower than the permissible limit (15 Pt-Co). Color in water is usually due to the presence of natural organic materials (such as humic substances), heavy metals, or some industrial pollutants (El Hammari *et al*., 2022 and 2023). Color removal occurs when these materials are either physically retained due to their large molecular size or adsorbed on the membrane surface (especially if the membrane has a large surface area).

Chemical Oxygen Demand (COD) and Biochemical Oxygen Demand (BOD_5)

The results showed a significant decrease in COD and BOD_5 values after filtration. COD decreased from 32 mg/L to 3 mg/L for the B5 membrane, a removal rate of 90.6%, which matches the permissible limit (3 mg/L). BOD_5 decreased from 19 mg/L to 2 mg/L for the B5 membrane, a removal rate of 89.5%, which is within the permissible limit (2 mg/L). This decrease reflects the membranes' ability to partially retain dissolved and colloidal organic materials, as well as their near-complete retention of microorganisms (bacteria), since bacterial size (typically 0.5-5 µm) is much larger than the membranes' pore size. This indicates that the prepared membranes possess high biological removal efficiency in addition to physical and chemical removal.

Total Dissolved Solids (TDS)

No significant change was observed in TDS values after filtration, with values remaining around 940-947 mg/L, which is below the permissible limit (1200 mg/L). This is completely expected because the operating mechanism of these membranes relies on size exclusion or microfiltration, and they are not designed to remove dissolved ions (such as sodium, potassium, and chloride salts), which are in the ionic size range (less than 1 nm). To remove these salts, membranes with finer porosity are needed, such as nanofiltration or reverse osmosis membranes. In general, these results are consistent with previous studies conducted on ceramic membranes prepared from natural materials or industrial wastes (Samadi *et al*., 2022; Goswami *et al*., 2022; Sawunyama *et al*., 2024), and confirm the effectiveness of these membranes in improving water quality, especially in removing turbidity and organic and biological pollutants. The B5 membrane (with 5% boric acid addition) is considered the best performer in balancing acceptable mechanical properties, high filtration efficiency, and compliance with standard specifications.

Conclusion

This research successfully demonstrated the feasibility of preparing low-cost inorganic ceramic membranes from Syrian fly ash (Class C) using boric acid as a binder and fluxing agent. The raw material was thoroughly characterized, confirming its classification as Class C according to ASTM C618 with a calcium oxide content of 16.80% and total acidic oxides of 62.10%, which provides self-cementing properties beneficial for the sintering process. X-ray diffraction analysis revealed that the fly ash consists mainly of quartz and calcite as primary crystalline phases, along with possible secondary phases such as hematite and mullite, and an amorphous glassy phase that enhances the pozzolanic activity and sinterability of the material.

The study investigated the effect of boric acid addition at different proportions (0%, 2.5%, 5%, and 7.5%) on the physical and mechanical properties of the prepared membranes after pressing and sintering at 900°C. The results showed that boric acid significantly influences the membrane characteristics, with the optimal performance achieved at 5% addition. At this proportion, the apparent porosity decreased from 38.75% to 26.80%, while bulk density increased from 1.58 g/cm³ to 2.08 g/cm³. The mechanical properties were substantially enhanced, with Vickers hardness increasing from 2280 MPa to 3670 MPa and compressive strength more than doubling from 15.8 MPa to 31.4 MPa. The permeability decreased from 0.045 Darcy to 0.009 Darcy, reflecting the denser structure resulting from improved sintering. However, increasing the boric acid content to 7.5% caused partial melting and deformation of the samples, confirming that 5% represents the optimal balance between enhanced properties and structural integrity.

The prepared membranes demonstrated excellent performance in drinking water treatment applications when tested on real water samples from a well at the University of Aleppo. The B5 membrane (containing 5% boric acid) successfully reduced turbidity from 12.80 NTU to 2.50 NTU, achieving a removal efficiency of 80.5%, while suspended solids decreased from 25 mg/L to 3 mg/L with 88% removal. The membrane also showed remarkable efficiency in removing organic pollutants, with COD reduced from 32 mg/L to 3 mg/L (90.6% removal) and BOD_5 from 19 mg/L to 2 mg/L (89.5% removal), bringing all these parameters within the limits specified by the Syrian drinking water standards. The color value was also significantly improved, decreasing from 12 Pt-Co to 4 Pt-Co. As expected for microfiltration membranes, no significant reduction in total dissolved solids was observed, which is consistent with the size exclusion mechanism of these membranes that cannot retain dissolved ions.

The findings of this research confirm that Syrian fly ash from the Banias Refinery represents a promising and economically viable raw material for producing effective ceramic membranes for water purification applications. This approach achieves a dual objective: the environmentally beneficial recycling of industrial waste that would otherwise require disposal, and the production of high-value-added filtration materials that can contribute to solving local water quality challenges. The ability to control the membrane properties by adjusting the boric acid content and sintering conditions provides flexibility in tailoring the membranes for specific applications. Future work could focus on scaling up the production process, investigating the long-term stability and fouling resistance of these membranes, and exploring their applicability to other types of water and wastewater treatment scenarios.

Acknowledgement

The authors would like to thank the University of Aleppo for providing the necessary facilities and support to complete this research.

Disclosure statement: *Conflict of Interest:* The authors declare that there are no conflicts of interest.

Compliance with Ethical Standards: This article does not contain any studies involving human or animal subjects.

References

Abdullayev A., Bekheet M.F., Hanaor D.A.H., Gurlo A. (2019) Materials and applications for low-cost ceramic membranes, *Membranes*, 9(9), 105. https://doi.org/10.3390/membranes9090105

Adewuyi Y.G. (2021) Recent advances in fly-ash-based geopolymers: potential on the utilization for sustainable environmental remediation, *ACS Omega*, 6(24), 15532-15542. https://doi.org/10.1021/acsomega.1c00662

Agarwal A. *et al.* (2020) Synthesis, characterization and performance studies of kaolin-fly ash-based membranes for microfiltration of oily waste water, *J. Pet. Sci. Eng*., 194, 107475. https://doi.org/10.1016/j.petrol.2020.107475

Asif M.B., Zhang Z. (2021) Ceramic membrane technology for water and wastewater treatment: A critical review of performance, full-scale applications, membrane fouling and prospects, *Chem. Eng. J*., 418, 129481. https://doi.org/10.1016/j.cej.2021.129481

ASTM C618-19 (2019) Standard Specification for Coal Fly Ash and Raw or Calcined Natural Pozzolan for Use in Concrete, *ASTM International*. https://www.astm.org/Standards/C618.htm

Cui Z. *et al.* (2023) Preparation of porous mullite ceramic supports from high alumina fly ash, *J. Mater. Cycles Waste Manage*., 25(2), 1120-1129. https://doi.org/10.1007/s10163-022-01578-w

Das D., Kayal N. (2023) Influence of additive contents on the properties of SiC ceramic membranes and their performance in oil-water separation, *Int. J. Appl. Ceram*. Technol., 20(3), 1715-1729. https://doi.org/10.1111/ijac.14312

Dong Y., Wu H., Yang F., Gray S. (2022) Cost and efficiency perspectives of ceramic membranes for water treatment, *Water Res*., 220, 118629. https://doi.org/10.1016/j.watres.2022.118629

El Hammari L., Latifi S., Saoiabi S., Saoiabi A., Azzaoui K., Hammouti B., Chetouani A., Sabbahi R. (2022), Toxic heavy metals removal from river water using a porous phospho-calcic hydroxyapatite, *Mor. J. Chem.* 10(1), 62-72, https://doi.org/10.48317/IMIST.PRSM/morjchem-v10i1.31752

El Hammari L., Hamed R., Khalil A., Jodeh S., Latifi S., Saoiabi S., Boukra O., *et al*. (2023), Optimization of the Adsorption of Lead (II) by Hydroxyapatite using a Factorial Design: DFT and Molecular Dynamic, *Frontiers in Environmental Science*, 11, 1112019., doi: 10.3389/fenvs.2023.1112019

Friesen J., Sanne M., Khurelbatar G., van Afferden M. (2023) OCTOPUS principle reduces wastewater management costs through network optimization and clustering, *One Earth*, 6, 1227-1234. https://doi.org/10.1016/j.oneear.2023.08.005

Fu H. *et al.* (2022) Preparation, characterization and properties study of a superhydrophobic ceramic membrane based on fly ash, *Ceram. Int*., 48(8), 11573-11587. https://doi.org/10.1016/j.ceramint.2021.12.356

Gollakota A.R., Volli V., Shu C.M. (2019) Progressive utilisation prospects of coal fly ash: A review, *Sci. Total Environ*., 672, 951-989. https://doi.org/10.1016/j.scitotenv.2019.03.337

Goswami K.P., Pakshirajan K., Pugazhenthi G. (2022) Process intensification through waste fly ash conversion and application as ceramic membranes: A review, *Sci. Total Environ*., 808, 151968. https://doi.org/10.1016/j.scitotenv.2021.151968

Hammal A. (2023). Preparing new ceramic membranes from Syrian zeolite coated with silver nanoparticles to treatment wells water, *Baghdad Sci. J*., 20(6), 2187-2192. https://doi.org/10.21123/bsj.2023.7620

Hammal A. (2025). Preparation of geopolymer membranes using clay and some industrial wastes to remove the organic load of pharmaceutical wastewater, *BMC Res. Notes*, 18, article 232, https://doi.org/10.1186/s13104-025-07299-9

Hossain S.S., Roy P. (2020) Sustainable ceramics derived from solid wastes: a review, *J. Asian Ceram. Soc*., 8(4), 984-1009. https://doi.org/10.1080/21870764.2020.1815348

Huang J. *et al.* (2023) Effects of particle size on microstructure and mechanical strength of a fly ash based ceramic membrane, *Ceram. Int*., 49, 15655-15664. https://doi.org/10.1016/j.ceramint.2023.01.183

Jiang F. *et al.* (2018) Formation mechanism of high apparent porosity ceramics prepared from fly ash cenosphere, *J. Alloys Compd*., 749, 750-757. https://doi.org/10.1016/j.jallcom.2018.03.355

Jin Y. et al. (2020) Structure refinement of fly ash in connection with its reactivity in geopolymerization, *Waste Manage*., 118, 350-359. https://doi.org/10.1016/j.wasman.2020.08.049

Jones E.R., Bierkens M.F.P., Wanders N., Sutanudjaja E.H., van Beek L.P.H., van Vliet M.T.H. (2022) Current wastewater treatment targets are insufficient to protect surface water quality, Commun. *Earth Environ*., 3, 1-8. https://doi.org/10.1038/s43247-022-00554-y

Labidi A. et al. (2023) Coal ash for removing toxic metals and phenolic contaminants from wastewater: a brief review, *Crit. Rev. Environ. Sci. Technol*., 1-24. https://doi.org/10.1080/10643389.2023.2184598

Liang D. *et al.* (2021) Influence of dextrin content and sintering temperature on the properties of coal fly ash-based tubular ceramic membrane for flue gas moisture recovery, *J. Eur. Ceram. Soc*., 41(11), 5696-5710. https://doi.org/10.1016/j.jeurceramsoc.2021.04.056

Mushtaq F., Zahid M., Bhatti I.A., Nasir S., Hussain T. (2019) Possible applications of coal fly ash in waste water treatment, *J. Environ. Manage*., 240, 27-46. https://doi.org/10.1016/j.jenvman.2019.03.054

Obaideen K., Shehata N., Sayed E.T., Abdelkareem M.A., Mahmoud M.S., Olabi A.G. (2022) The role of wastewater treatment in achieving sustainable development goals (SDGs) and sustainability guideline, *Energy Nexus*, 7, 100112. https://doi.org/10.1016/j.nexus.2022.100112

Samadi A., Gao L., Kong L., Orooji Y., Zhao S. (2022) Waste-derived low-cost ceramic membranes for water treatment: Opportunities, challenges and future directions, *Resour. Conserv. Recycl*., 185, 106497. https://doi.org/10.1016/j.resconrec.2022.106497

Sawunyama L., Olatunde O.C., Oyewo O.A., Bopape M.F., Onwudiwe D.C. (2024a) Application of coal fly ash based ceramic membranes in wastewater treatment: A sustainable alternative to commercial materials, *Heliyon*, 10, e24344. https://www.cell.com/heliyon/pdf/S2405-8440(24)00375-X.pdf

Sawunyama L., Olatunde O.C., Oyewo O.A., Bopape M.F., Onwudiwe D.C. (2024b) Ceramic-polymer composite membranes: synthesis methods and environmental applications, *Ceram. Int*., 50, 5067-5079. https://doi.org/10.1016/j.ceramint.2023.12.089

Singh G., Bulasara V.K. (2015) Preparation of low-cost microfiltration membranes from fly ash, *Desalin. Water Treat*., 53(5), 1204-1212. https://doi.org/10.1080/19443994.2013.855678

Suresh K., Pugazhenthi G., Uppaluri R. (2016) Fly ash based ceramic microfiltration membranes for oil-water emulsion treatment: parametric optimization using response surface methodology, *J. Water Process Eng*., 13, 27-43. https://doi.org/10.1016/j.jwpe.2016.07.008

Wang C., Liu Y., Li H., Xu M. (2021) High value-added applications of coal fly ash in the form of porous materials: a review, *Ceram. Int*., 47(16), 22302-22315. https://doi.org/10.1016/j.ceramint.2021.05.070

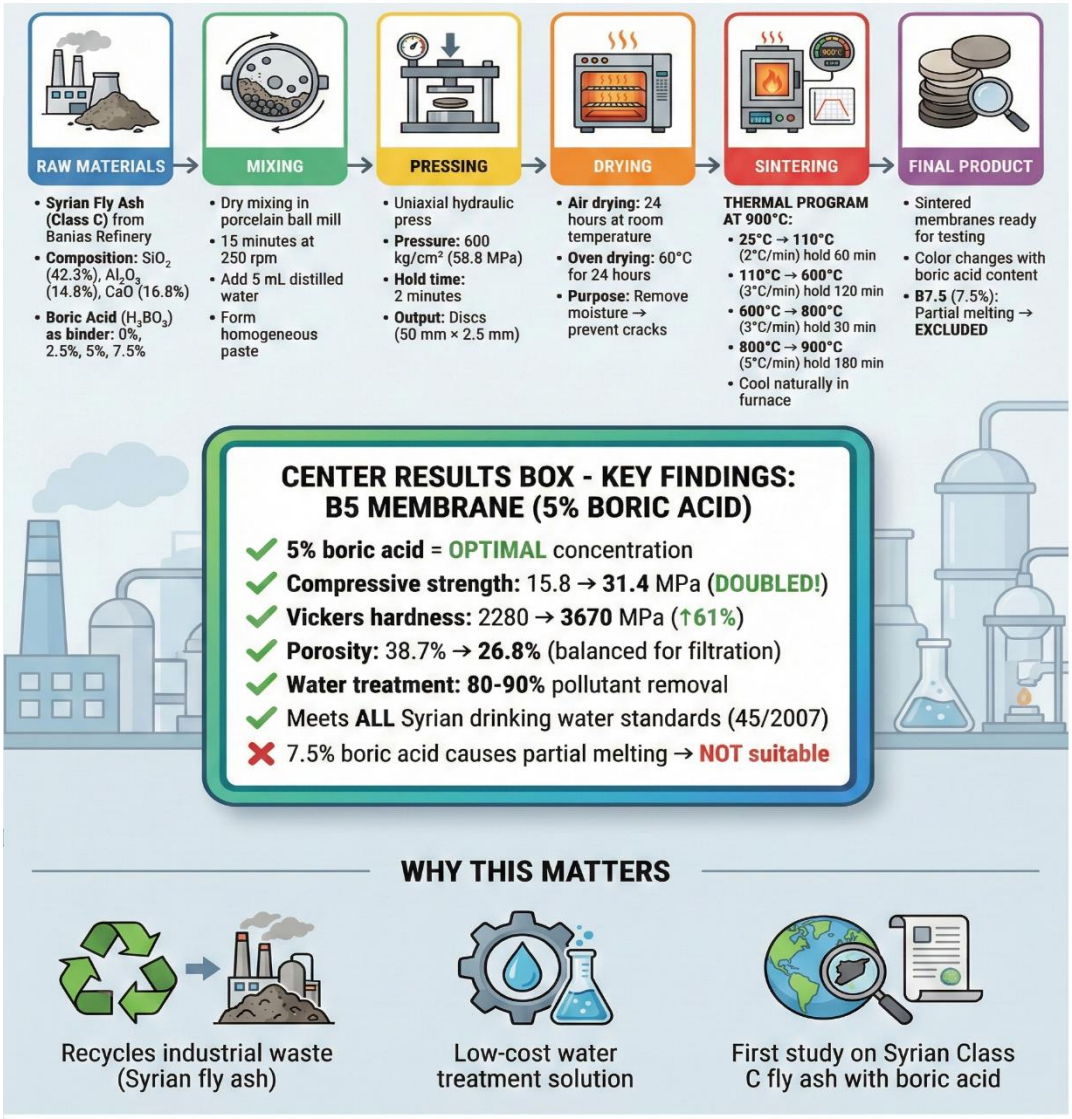

(2026); http://www.jmaterenvironsci.com